SIMULATION OF GRAPHENE SYNTHESIS ON FACETED SURFACE OF SILICON CARBIDE FOR HIGH CRISTALLINITY GRAPHENE STRUCTURES FORMATION

Nikolay I. Alekseyev, Viktor V. Luchinin

St.-Petersburg ElectroTechnical University LETI, http://www.eltech.ru
197376 St.-Petersburg, Russian Federation
nialekseyev@yandex.ru, luchinin@eltech-fel.ru

Abstract. **The silicone carbide SiC faceted surface is optimized with a viewpoint of producing high-crystallinity graphene with the possibly maximal bandgap. We considered the faceting folds, which appear in the course of splitting vicinal SiC (11−2n) face for the steps as the source of opening non-zero bandgap in the graphene. The structure with spatial period of ~30nm, where the lower estimation of ΔE_g gives 0.2÷0.25eV, is offered as optimal for the practice. An approach to practical production of this structure is estimated.**

Keywords: **graphene, silicon carbide, simulation of synthesis, facetiously surface, bandgap, vicinal face.**

PACS: 68.65 Pq, 81.15

Bibliography − 12 references *Recieved 13.09.2015*

RENSIT, 2015, 7(2):135-144 **DOI: 10.17725/rensit.2015.07.135**

Contents

1. INTRODUCTION

It is known that the most potentially manufacturable graphene production method for microelectronics applications is the sublimation growth on the silicon carbide *SiC* surface. But do far this method did not allow a uniform defect-free graphene fragment of large area to be obtained. Such a fragment, even without a non-zero bandgap is important for applications in optoelectronics.

High commensurability of the crystal lattices of the graphene and that of *SiC* (e.g., in the $(6\sqrt{3}\times6\sqrt{3})R30°$ superlattice [1]) should, as it is natural to think, promote the formation of large area steady graphene structures, but it does not. Thus, the typical width of the terrace−like graphene structures grown on *Si*–face of an optimally prepared *SiC* substrate [2], does not exceed (1÷2) μm. As to the *SiC* substrate, prepared by standard chemical-mechanical polishing (CMP), it allows a mosaic structure of graphene fragments of still smaller size.

This result is shown in Supplement 1 to be of quite universal character and stems from rather simple estimates.

The researches related with obtaining graphene fragments of confined area with the both non-zero bandgap ΔE_g and high carrier mobility, have a different focus, but also meet essential problems. These researches concentrate around two principal ideas − the synthesis of graphene nanoribbons *NR*, and stretching the graphene. Now we discuss the third and the most natural (to our opinion) way to achieve the principal requirements to the operating graphene structure: a certainty in the number of layers, the bandgap $\Delta E_g \neq 0$, and high carrier mobility).

The model problem considered in this paper is as the follows. We suppose that we have a *SiC* -faceted surface, obtained as a result of cutting

solid crystal *SiC* along a plane beveled with relation to the *Si*-face (0001) (or to the *C*-face (000–1)), e.g., the plane (11–2*m*), and subjected to subsequent anneal at the temperature below the graphene synthesis temperature. This processing allows the *SiC* faceted surface to be formed with a spatial period

$$L \geq h/\sin\alpha \quad (1)$$

where h is the period of the *SiC* polytype along the axis [0001], α is miscut angle to the plane (0001) (or (000−1)). The spatial period L consists of the fragment of the plane (0001) ("horizontal" part of the step) and of the declined part of the step (**Fig. 1**).

The goal consists in finding the optimal character of the faceting for achieving the maximum possible bandgap width and high-quality surface, providing high carrier mobility, at the same time.

It should be noted first of all that the estimate (1) is only applicable if the angle α is not too large. With α > (4÷5)° the coarsening of the structure during the anneal stage prevents from producing highly periodical structure and the quality of the faceted *SiC* surface decreases drastically [3].

Therefore, in the future estimates the angle α is considered sufficiently small (and the the length L is large, respectively) so that it contains a large number of the graphene lattice constants. Suppose, then, that when the temperature reaches the level sufficient for the sublimation graphene synthesis, the graphene structure reproduces the shape of the downlaying *SiC* surface (Fig. 1), formed before the formation of graphene. The reasonability of so strong preposition is considered in "Discussion".

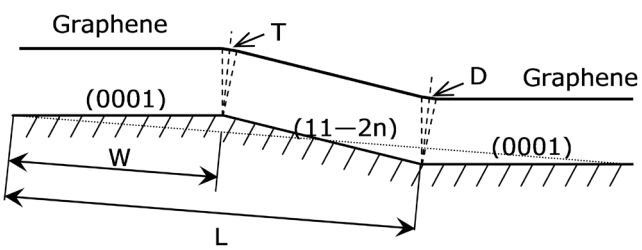

Fig. 1. *The graphene, obtained by sublimation of the Si-component from SiC surface (upper broken line), and the SiC surface after the formation of graphene – the lower broken line. Points "T" (top) and "D" (down) are the graphene folds at the upper edge of the top of the declined part of the step and at the bottom of the step.*

Herewith over the both projecting edge of the *SiC* surface (the point *T* (top) in Fig. 1) and the internal edge of the declined part of the step (point *D* (down) in Fig. 1) the graphene surface folds with a certain curvature arise. A periodic structure is Formed similar to the graphene nanoribbons *NR* (nanoribbons) to provides a finite bandgap width.

Compliance of this simple model picture with real experiments on the graphene growth on the faceted *SiC*−surface is discussed in the section "Discussion".

2. CALCULATION METHOD AND RESULTS

We chose the formalism of Green's functions in nodal representation as a research method. It started to be used efficiently by S.Yu.Davydov and described as applied to the flat graphene on the *SiC*-substrate in [4].

The Green's function $\hat{G}$ is known to be determined by the Hamiltonian $\hat{H}$

$$\hat{G} = (E - \hat{H} - i_0)^{-1} \quad (2)$$

and the pole of this function determines the eigenvalue of the energy E.

In the nodal representation the function $\hat{G}$ turns into the matrix

$$G_{mn}(E) = \langle \psi_m | (E - \hat{H} - i0)^{-1} | \psi_n \rangle, \quad (3)$$

where the Vannier functions are the brackets: $\langle \psi_m |$ и $| \psi_n \rangle$, m and n are the lattice nodes [5].

Remarkable properties of the nodal representation are that

– the set of the equations for these functions is a system of algebraic equations;

– in the areas where there is a strict periodicity, the diagonal and non-diagonal Green's functions are linked by simple relations. For example, in two-dimensional crystal lattice

$$G_{mn} = G_{mm} exp(i\mathbf{k}(\mathbf{r}_n - \mathbf{r}_m)). \quad (4)$$

The equation (4) is valid for the nodes m,n, placed from each other at a distance of a whole number of the lattice constants. If the nodes are

separated by a smaller distance but are physically equivalent, this relation is valid as well. For example, in **Fig. 2** the functions G_{10} and G_{00} are related with each other as $G_{10} = G_{00}exp(-i(k_x a/2 + k_y a\sqrt{3}/2))$ where the node "1" is separated from the node "0" by 1/3 of the lattice constant.

The basic equation for the Green's function determination in the nodal representation is the Dyson's equation. In the case of the infinite graphene and by taking into account the nearest neighbors only:

$$G_{00} = g_{00} + g_{00}(V_{01}G_{10} + V_{02}G_{20} + V_{03}G_{30}), \quad (5)$$

where $\gamma = V_{01}$, V_{02}, V_{03} are the hopping elements between the nearest neighbors (Fig. 2), G_{10}, G_{20}, G_{30} are the off-diagonal elements of the Green's functions matrix, g_{00} − is the diagonal element of the "seed" Green's functions matrix.

The Green's function of individual carbon adatoms, not interacting one with another, on a *SiC* − substrate, or the Green's function of free carbon atoms arranged in a "correct" positions of the graphene mesh can be selected as these "seed" elements. Since we are interested in achieving a sufficiently wide band gap, the contribution to ΔE_g, associated with the *SiC*-substrate, is assumed negligible. The very graphene is considered as a free periodically deformed structure. Then $g_{00} = 1/E$.

Suppose, then, that the external folds (the points "*T*" in Fig. 1) and the internal folds (points «*D*») of the graphene surface have the same curvature. This curvature leads to a local decrease in the matrix element γ (γ → γ') and to changing the Green's function as compared with the undistorted graphene. Assume first that the faceting breaks the steps to horizontal parts and the declined ones with equal lengths (i.e., the horizontal part width is $W = L/2$). Then the effective period of the problem is halved as compared to the spatial period of the *SiC*-structure.

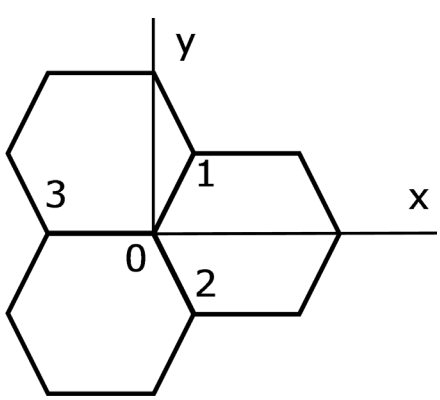

Fig. 2. *A fragment of an infinite flat graphene around the node "0" and its nearest neighbors, contributing to the Dyson's equation.*

In the **Fig. 3**, which shows the periodically distorted graphene in the drawing plane, the fold area is shown in bold lines. We also give the numbering of the lattice nodes used in the subsequent formulas. The distance between the lines of distortion (vertical border lines of the "armchair" type in Fig. 3) is $n\bar{a}$ ($n \in Z$), whilst the real graphene structure period is $2n\bar{a}$ ($\bar{a} = a\sqrt{3}$ is the period of the structure in the "zigzag" direction, $a = 0.142nm = 0.246nm$ – is the C-C bond length).

Note that in the Fig. 1 the tops of the faceted *SiC* surface under the graphene (points "*T*") are shown as the "acute" tops. Given that the distance between the graphene and the *SiC* is approximately correspondent with the Van der Waals (VdW) interaction length, we obtain that the distortion of the matrix element γ extends no longer than one *C-C* bond from the folding point. The consideration for the case of the downlaying *SiC*− surface being rounded is briefly concerned on in the section "Discussion"

The starting Dyson's equation for the node "0" has the form

$$G_{00} = g_0 + g_0(\gamma G_{00}\exp(i\mathbf{k}_y\mathbf{a}) + V_0 G_{10}(1+\exp(i\mathbf{k}_x\bar{a}_x))), \quad (6)$$

so for the nodes whose distances from the point "0" are the even and the odd number of halves of lattice constant $\bar{a}/2$, respectively:

$$G_{2m,0} = g_{00}(V_{2m-1}G_{2m-1,0} + V_{2m}G_{2m+1,0} + \gamma G_{2m}\exp(+i\mathbf{k}_y a)), \quad (7)$$

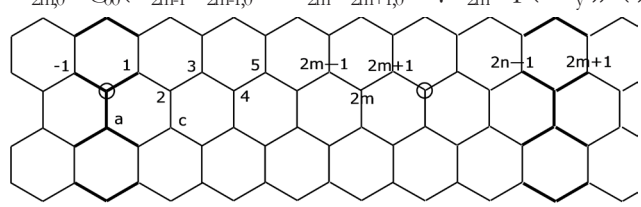

Fig. 3. *The half-period of "zigzag" graphene structure over the faceted SiC surface. The bold lines – are the areas of the graphene folds over the SiC surface. The points "0" and «2n» are identical with the points "T" and "D" in Fig. 1.*

$G_{2m+1,0}=g_{00}(V_{2m}G_{2m,0}+V_{2m+1}G_{2m+2,0}+\gamma G_{2m+1,0}\exp(-i\mathbf{k}_y a))$, (8)

where the denotion $V_0 \equiv V_{01}$, $V_1 \equiv V_{12}$ etc. for the matrix elements of the interacting atoms is introduced for brevity.

In the middle of the faceted graphene structure period

$G_{2n,0} = g_0\gamma(G_{2n-1,0} + G_{2n+1,0} + G_{2n.0}\exp(+i\mathbf{k}_y a))$. (9)

Given the equivalence of the nodes 2n−1, 2n + 1, we find that

$G_{2n+1,0} = G_{2n-1,0}\exp(-i\mathbf{k}_x \bar{a})$,

$$G_{2n,0} = G_{2n-1,0}z_{2n-1};\quad z_{2n-1} = \frac{1+\exp(-ik_x\bar{a})}{\varsigma-\exp(ik_y a)}; \qquad (10)$$

(the parameter ς is defined herein as $\varsigma = 1/\gamma g_{00}$).

It is easy to install then the shape of the recurrence relations for the multipliers z which bind the functions $G_{2n—1,0}$, $G_{2n—2,0}$, etc.:

$G_{2n-1,0} = G_{2n-2,0}z_{2n-2}$, $z_{2n-2} = (\varsigma - (z_{2n-1} + \exp(-i\mathbf{k}_y a))^{-1}$, (11)

$G_{2n-2,0} = G_{2n-3,0}z_{2n-3}$, $z_{2n-3} = (\varsigma - (z_{2n-2} + \exp(-i\mathbf{k}_y a))^{-1}$, (12)

$z_1 = G_{10}/G_{00} = (\gamma'/\gamma)(\varsigma - (z_2 + \exp(-i\mathbf{k}_y a))^{-1}$. (13)

Taking then the Dyson's equation at the point "1":

$G_{1,0} = g_{00}(\gamma' G_{00} + \gamma z_2 G_{1,0} + \gamma G_{10}\exp(-i\mathbf{k}_y a))$ (14)

we obtain the dispersion relation, written in "canonical" shape:

$G_{00} = g_{00} + \gamma g_{00}G_{00}f$ or

$G_{00}^{-1} = g_{00}^{-1} - \gamma f$ (15)

with $G_{00}^{-1} = 0$. In our case the function

$f = \exp(ik_y a) + (\gamma' z_1/\gamma)(1 + \exp(ik_x \bar{a}))$. (16)

It is known that if the "seed" Green's function g_{00} is real, the complex function f should be replaced by $\pm|f|$, and then the dispersion equation takes the form:

$g_{00}^{-1} = \pm\gamma|f|$ (17)

It is known, further, that for the undistorted graphene

$$f(\mathbf{k}) = \sqrt{3+2\cos(\sqrt{3}k_y a)+4\cos(\sqrt{3}k_y a/2)\cos\left(\frac{3}{2}k_y a\right)}$$

[6] and the zeroes of this function allow the Dirac points **K** and **K'**, fundamental for the theory of graphene: f(**K, K'**) = 0.

In the case of f in the form of (16) we must take quantities k_x, k_y which are correspondent with one of the points **K, K'** of undistorted graphene at $\gamma'/\gamma \to 1$ and $\varsigma \to 0$. This allows not to build the dispersion relation E(**k**) when finding ΔE_g in the faceted structure, but watch how the tops of the Dirac cone go apart only, depending on the period of the structure and the factor γ'/γ. It is not difficult to trace that with $\gamma'/\gamma \to 1$, $\varsigma \to 0$ one of the solutions to (16) in the first quadrant of the plane (k_x, k_y) is the point $k_x\bar{a} = 4\pi/3$, $k_y a = 0$. It is correspondent with one of the Dirac points and was selected to build the dependencies $\Delta E_g(\gamma'/\gamma, L)$.

The dependencies are shown in **Fig. 4**. The abscissa is the factor $t = W/(\bar{a}/2)$ − the doubled number of the lattice constants in the "zigzag" direction. The Fig. 4 is correspondent with the model structure with the period of $W = L/2$, i.e. the half-period of the faceting (in Fig. 3 t = 7). The ΔE_g dependence on t is built with three ratios γ'/γ: 0.9, 0.95, and 0.98. The calculation of the real ratio γ'/γ is described in the Supplement 2. It is based on the estimation of the binding energy change in some "zigzag" nanotube. Its radius was supposed to be equal to the graphene curvature radius in the folding point, i.e. to the graphene-*SiC* VdW-binding length. The closest to the reality is the curve 3 which is correspondent with to $\gamma'/\gamma = 0.98$.

It is seen from the Fig. 4 that the "enlightenment" periods of the structure are proportional to $3\bar{a}/2$, as well as for the graphene

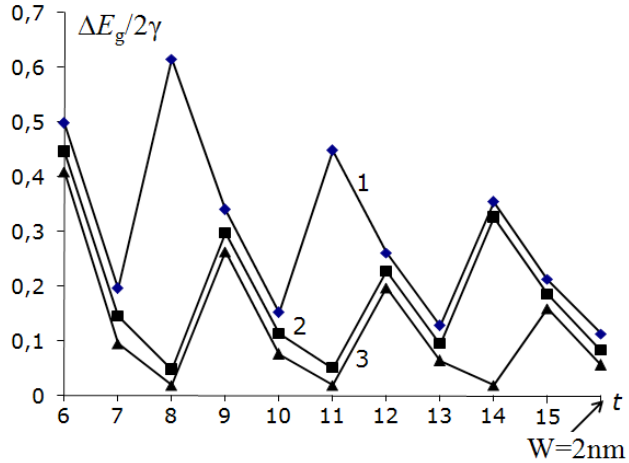

Fig. 4. *The dependence of the bandgap on the faceted structure half period, given that $W = L/2$ (when the length of the horizontal and declined parts of the steps are equal). For polygonal lines 1, 2, 3 γ'/γ is: 1 – 0.9, 2 – 0.95, 3 – 0.98; γ' – altered value of the constant γ at the fold point.*

nanoribbons *NR*. With the appropriate widths of the *NR* the bandgap disappears. In our case, the distortion in the faceted structure is a small fraction of the maximum distortion, which is correspondent with the breakage of the structure. Such breakage takes place in *NR* where the gap ΔE_g falls to zero. As to the maxima of the curves $\Delta E_g(t)$, they are easy to be related with the simple estimate: $\Delta E_g = \hbar v F/W$ [6]; $\Delta E_g[eV] \approx 4/W[nm]$. So, with $t = 15$ and a ratio $\gamma'/\gamma = 0.98$ the model structure period is $W \approx 15 \cdot 0.246/2 = 1.85$ *nm*, the ratio $\Delta E_g/2\gamma$ in Fig. 4 is $\Delta E_g/2\gamma \approx 0.17$, and $\Delta E_g = 1eV$. The simplest estimate gives notably greater value: $\Delta E_g = 2eV$, as it should be.

3. DISCUSSION

Until now, when trying to create the graphene at the *SiC* face, declined with relation to the silicon-(0001) (or carbon (000−1)) faces, multi-layered graphene always formed. This result is a consequence of the fact that silicon evaporates faster at the declined part of the step than it does at the horizontal part, and while the nucleus of the graphene (graphene island) "grinds" the top- and the bottom parts of the step (points "*T*" and "*D*" in Fig. 1 and 5), a nucleus of a new graphene layer has time to appear under the existing one [7] − **Fig. 5**.

On the other hand, it is known that when growing the graphene on singular carbon faces, the upper layer (i.e. the very first graphene layer since the nucleation moment) is rotated with respect to the lower-laying layers of the *Si, C* atoms, which fact defines a regular disorder orientation of the graphene layers (rotational stacking faults) [1].

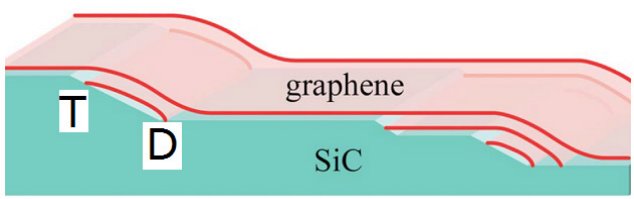

Fig. 5. *Scheme of the multilayer graphene formation at declined face of SiC, observed and described qualitatively in* [7]. *The points "T" and "D" are the basic points of the starting graphene island on the declined part of the step formed on SiC in the course of faceting.*

In the system of such graphene layers, every of which is rotated in relation to the previous one, every layer behaves itself as an independent monolayer graphene. If the property of rotational disorder persisted for growing graphene on vicinal *SiC* face, the multilayered nature of the graphene would have been insignificant. It would be enough then to carry out all the necessary technological procedures with the upper layer only.

Earlier, when simulating the graphene synthesis on the singular *SiC*−faces with semi-empirical quantum chemistry methods (SEQCM) in the package *HyperChem*, we observed the rotational disorder formation at the level of the detailed assembly kinetics [8, 9]. During this simulation we watched, in particular, the 3x3 reconstruction which immediately precedes the formation of graphene in the experiments on the *C*-face [1]. However, in the experimental reconstructions 3×3 the details of the atomic arrangement are not clearly identified, and various models are possible.

In our simulation the nontrivial rotation of the graphene with relative to the *SiC* substrate is seen just at the 3×3 reconstruction stage. This stage is correspondent with the completed destruction of the second atomic layer of the *SiC* and is reduced to the formation of the graphene islands comprising 18 carbon atoms (**Fig. 6**). Low symmetry of the structure of this island leads to its rotation from the down-laying *SiC*

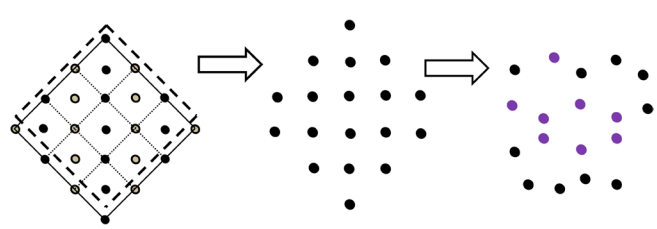

Fig. 6. *Detailed scheme of how the singular carbon face of SiC is rebuilt to the graphene. The left drawing is the 2×2 reconstruction of carbon atoms in the upper layer of SiC. The atoms C which belong to the upper layer of the SiC atoms, are shown by black circles, the atoms of the second layer are shown by gray circles. Bold dotted line highlighted the future 3×3 reconstruction cell, comprising the atoms of both the first and the second layers. The central drawing shows the carbon atoms of the same cell in the same color, without dividing them into layers. The cell includes 18 carbon atoms. The right drawing is the schematic of connection the atoms of the unit cell to the graphene island.*

layers. At this stage the island is still covalently bound with the *SiC*.

When the graphene islands laterally stack one with another the covalent interactions between the graphene and the *SiC* changes to VdW-interactions but the rotation of the islands with respect to the *SiC* remains.

We put the problem to follow the similar (or different) behavior of the graphene on the vicinal faces, sloped with respect to the carbon face (000−1). It was found that the stacking rotation fault, similar with that on the singular carbon faces, is observed in this case as well. Moreover, if the first monolayer islands have typical rotation of 2.2° with respect to any of the three equivalent "zigzag" directions on the (000−1) plane [1] on the singular face (000−1), there is the only preferred direction on the vicinal *SiC* face, laying in parallel with the folding lines ("*T*" and "*D*" in the Fig. 1).

The starting graphene islands which arise at the declined parts of the steps (**Fig. 7**), are rotated in relation to this direction. In the course of the transfer of the islands from these declined parts to the horizontal parts (000−1) this orientation is saved. Therefore the lateral stacking of the islands, emerged on the declined parts of different steps, should lead to the formation of a whole single graphene monolayer instead of the mix of differently oriented islands.

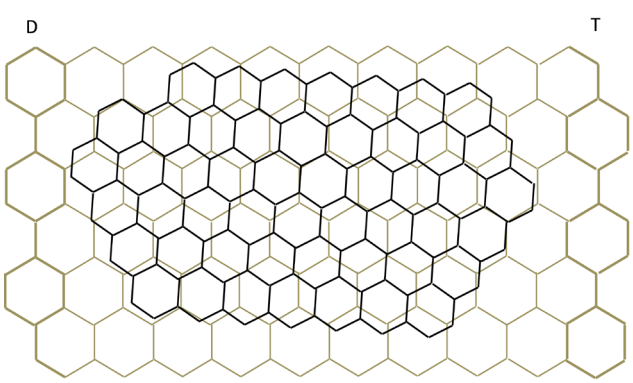

Fig. 7. *Graphene island over the declined part of the SiC faceted structure. The larger mesh SiC is shown in gray, without separating the atoms to carbon and silicon, the smaller mesh (graphene) is shown in black. Bold vertical lines on SiC are the top of the step (line "T") and deepening of the step (line "D"−down), respectively.*

Consequently, the unique properties of the graphene, emerging on the infinite singular carbon face (000−1) in the form of the graphene island packs of relatively small area must be maintained on vicinal *SiC* face for the whole graphene monolayers. In particular, the top layer must be electrically separated from the down-placed layers, i.e. it is equivalent to the graphene monolayer. For such monolayer the folds at the edges of the steps provide a non-zero bandgap width (maintaining at the same time high carrier mobility) and his bandgap can be calculated as a function of the vicinal angle (as in Fig. 4).

However, the upper graphene layer of high crystallinity, deformed along the folding lines only, can only emerge if the singular parts of the steps and declined parts between them are not wider than the characteristic size of the perfect graphene fragments at the singular *C*-faces of *SiC*, observed experimentally. This width has the order of 0.5 μm [10] and is easily achieved with the cutting angle greater than 10.

Certainly, this estimate has no practical value, as the cutting angle required to obtain a sufficient band gap is much larger, and the necessary terrace width is much smaller.

As for the upper estimate of α, it is determined by the technology. As already said, the faceting quality of the original *SiC* surface is provided at $\alpha \leq (4\div5)°$. Let $\alpha = 3.50$. Then for the polytype 4*H-SiC* the faceted structure period is $L \approx 30$ *nm*. With so large period the existence of the discrete widths of "enlightenment", following with a periodicity ΔL of $3\bar{a}/2$, has no matter. Even a small variation in the period should lead to localization and smoothing the $\Delta E_g(L)$ dependence. With $L = 30$ *nm* and $W = 15$ *nm* the calculated ΔE_g is about 0.12 *eV*.

In fact, this estimate is lower one. The calculation with $W \neq L/2$ shows the maximum at W, intermediate between zero and the point $L/2$. At $L = 30$ *nm* $\Delta E_g = 0.17$ *eV*. However, the ratio W/L is determined self-consistently in the course of annealing. Let us assume, then, that in view of delocalization one can rely on the band gap of about 0.2 *eV*.

Consideration of the smoothed tops (instead of the acute ones, described above), does not improve the above estimate. In this case the described model was applied in the following way. The semi-period of the faceted structure from the point "*T*" to the point "*D*" was divided by three parts: the central part, which is correspondent with the undistorted graphene, and two margin regions, which contain some number of the graphene structure periods and carry a fixed folding curvature.

As already said, the resulting solution detects no features.

The more important fact is that the experimentally observed spatial period of the structure increases drastically in the course of the transfer from the faceted surface of the *SiC* to the graphene. The reason is quite clear.

In order to form a continuous graphene layer over the edge of a step, a larger number of the *SiC* layers should be destroyed than for the graphene formation over the central regions of this step. Therefore the edges of the steps can disappear at all and the *SiC* surface under the formed graphene is subjected then to a new faceting process which reestablish the spatial period.

Though, it is clear that if a single graphene island has time to be formed at the declined part of the step and no island – at the horizontal part (0001) (or(000−1)), the factor of dramatic increase in the spatial period has no time to be developed. A system of the graphene nanoribbons, separated by insulating strips of *SiC* is formed is this case.

If the sublimation process goes on a bit longer to allow a substantial number of the graphene layers to be formed, the alternation of the graphene strips arises, in which the adjacent strips have the greater- and the smaller number of the graphene layers, and different widths.

The both situation are interesting for the applications: the first one – for the formation of the structures with $\Delta E_g \neq 0$, the second one enables the possibility of the THz radiation gain by analogy with the system of alternating graphene- and metallic strips [12].

But the number of the layers which are formed (one or many) within a reasonable time-scale of the experiment is determined by the temperature. The calculation of the *SiC* evaporation rate at different temperatures at the vicinal *C*−face (similar with the calculation conducted for *Si*- and *C*-singular faces in [9]) enable reasonable anneal temperature to be chosen for the yield of a regulated preset number of the graphene layers.

So, the calculated simulation of the graphene on vicinal faces of *SiC*, combining the Green's functions method and the use of SEQCM to determine the parameters of the model, allows a range of other physical ideas to be offered and accessed.

SUPPLEMENT 1. MAXIMAL AREA OF HOMOGENEOUS MONOLAYERED GRAPHENE FRAGMENT

We assume that during the sublimation of the silicon component from the *Si*-face (0001) of *SiC* a continuous flat infinite graphene layer is formed reconstructed by the scheme $(6\sqrt{3}\times6\sqrt{3})R30°$ with respect to the *SiC* mesh (**Fig. 8**). Consider its square fragment with the area $L\times L$. The sides of superstructure cells (gray in Fig. 8) include 13 graphene cells and the bonds in them are stretched ~0.14% as compared to

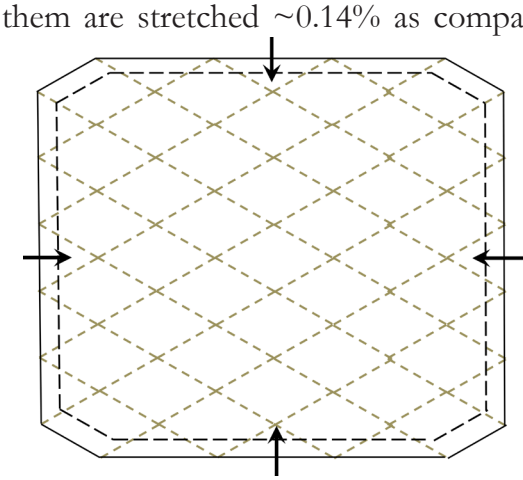

Fig. 8. *A fragment of the graphene surface, reconstructed by the scheme $(6\sqrt{3}\times6\sqrt{3})R30°$ (outer square, solid line, superstructure units form a rhombic lattice, marked in gray) and its conversion to the fragment of a quasi-free graphene, its chemically binding with SiC is only partial.*

the graphene undistorted bonds. Then at some area of the fragment a separation from the surrounding graphene becomes profitable and the observed area turns into a free graphene flake. This occurs when the energy gain overlaps the energy loss.

The gain $\Delta E^{(1)}$ is connected with a disappearance of the strained *C-C* bonds in the graphene mesh. It is proportional to the total number of bonds in the graphene scrap of the area $L\times L$, free of stretching tension:

$$\Delta E^{(1)} = B\Delta E_1 = (3/2)N_{at}^{(1)}\Delta E_1 = 3\frac{L^2}{s_6}E_1,$$

where $B \approx 3N_{at}^{(1)}/2$ is the number of *C-C* bonds in the flake, $N_{at}^{(1)}$ is the number of atoms in it, $s_6 = 3a^2\sqrt{3}/2$ is the graphene cell areas, ΔE_1 is an additional strain energy per a bond in the stretched graphene

The energy loss is due to two factors:

– appearance of carbon atoms with uncompensated valence bonds at the edge of the flake

$$\Delta E^{(2)} = \frac{4L}{\overline{l}_{za}}E_{rad},$$

where E_{rad} is the energy per one absent valence bond – the radical (*rad.*), $\overline{l}_{za} = (l_{arm} + l_{zigz})/2$ – the average distance between the radicals along the lines of *armchair* and of "*zigzag*" in the flake: $l_{\text{arm}} = 3a/2$ и $l_{zigz} = a\sqrt{3}$;

– disappearance of the atoms, most strongly associated with down-layered silicon atoms of

$$\Delta E^{(3)} = \frac{L^2}{s_{\text{sup}}}\Delta E',$$

where $\Delta E'$ is the difference between the binding energies of the *C-Si* bonds between the carbon atoms arranged in a superlattice $(6\sqrt{3}\times 6\sqrt{3})R30°$ node and the carbon atoms located over the *Si*-face in some averaged position, $s_{\text{sup}} = (1/2)a^2_{\text{sup}}\sqrt{3}$ is the area of the cell superstructure ($a_{sup} = 13\bar{a}\sqrt{3}$ – is the side of the superstructure cell).

From the condition $\Delta E^{(1)} > \Delta E^{(2)} + \Delta E^{(3)}$, we have then

$$\frac{L}{\overline{l}_{za}} > \frac{4E_{rad}}{3\Delta E_1}\frac{\overline{l}_{za}^2}{s_6}\left(1 - \frac{3\Delta E'}{4E_{rad}}\frac{s_6}{s_{\text{sup}}}\right)^{-1}.$$

The bond stretching energy was evaluated on the basis of the Brenner potential [11] – the most perfect potential in molecular mechanics for carbon-hydrogen systems.

At low relative stretching $\Delta E_1 = D(\beta^{(e)}R_1^{(e)}\xi)^2$, of the *C-C* bond $\Delta E_1 = D(\beta^{(e)}R_1^{(e)}\xi)^2$, where the numerical value of the model parameters product $\beta^{(e)}R_1^{(e)} = 2$, $D = 6.31eV$.

The value of E' was determined by the SEQCM AM1 from the *HyperChem* package. We took a structure with an area a bit larger than the unit cell $(6\sqrt{3}\times 6\sqrt{3})R30°$. It included two layers of atoms *SiC* (actually the polytype 2*H*) and the graphene fragment over it. The positions of the *Si, C* atoms of *SiC* considered then as the fixed ones. First the free graphene fragment (free from the reconstruction cell) was considered and the optimal distance between the *Si*-atoms in the specified nodes of the reconstruction $(6\sqrt{3}\times 6\sqrt{3})R30°$ and graphene atoms, closest to them, was found. Then these *C*-atoms were exactly installed to the nodes, their coordinates were fixed, and an optimization of the position of all other atoms in the graphene was found.

The energy E_{rad} was supposed $E_{rad} = 2.5eV$ – which value is the half of the *C-C* covalent binding energy. The parameter ξ in the $6\sqrt{3}$ reconstruction is $\xi = 0.1\%$. Then $\Delta E_1 = 5\cdot 10^{-5}$eV and $L/\overline{l}_{za} \approx 1.7\cdot 10^5, L \approx 40\mu m.$

This is about 40 times greater than the size observed experimentally. It follows that the infinite graphene, reconstructed according to the scheme $(6\sqrt{3}\times 6\sqrt{3})R30°$, is not realized to be defective at the stage of the reconstruction already. The more detailed analysis shows that the graphene islands can be laterally stacked with each other without forming defects, up to the size of (2÷4) μm, which quantity is only a few times greater than the experimental result.

SUPPLEMENT 2. BINDING ENERGY CHANGE ESTIMATION IN THE "ZIGZAG" NANOTUBE AS COMPARED WITH THE INFINITE GRAPHENE

We parameterized the total energy of the zigzag nanotube as the follows.

Let the nanotube has n rows of hexagons and m hexagons along the circumference. Then

− the number of vertical bonds (i.e. the bonds, parallel with the nanotubes forming line) is mn. Let the energy module of such bonds is $E_1(m) > 0$;

− the number of external bond (i.e. bonds, one end of which is radical) is 4 m. Let the energy module of such bonds is E_2;

− the number of the required bonds (distorted bonds arranged with an angle to the both generatrix and the cross section of the nanotube) is $2m(n-1)$. Let the energy of such bonds is $E_0 = E_0(m)$.

Then, the binding energies of the nanotubes with the number of rows n, $n+1$, $n+2$ are

$$E_{(n)} = E_0 2m(n-1) + E_1 mn + E_2 4m,$$
$$E_{(n+1)} = E_0 2mn + E_1 m(n+1) + E_2 4m,$$
$$E_{(n+2)} = E_0 2m(n+1) + E_1 m(n+2) + E_2 4m,$$

so that the energy differences are

$$\Delta E_{(n)} = E_{(n+1)} - E(n) = E_0 2m + E_1 m,$$
$$\Delta E_{(n+1)} = E_{(n+2)} - E_{(n+1)} = E_0 2m + E_1 m,$$

should not depend on n. When calculating with using SEQCM package *HyperChem* (AM1 method), this fact is performed with a high accuracy, and $\Delta E_{(n)}$ can be considered for any number of the rows n. The factors E_0 and E_1 can not be determined separately from the difference $\Delta E_{(n)}$. However, the bonds with the energies E_0 and E_1 are slightly different in the lengths and in the valence angles formed by the bonds of their end atoms with their neighbour carbon atoms.

These factors are taken into account in Brenner potential. Substituting the distances and the angles calculated in *HyperChem*, to the expression of this potential, we obtain the ratio E_0/E_1. Then the absolute value of E_1 is different from the binding energy in a flat infinite graphene by less than 0.3%. On the other hand, the difference E_0/E_1 from 1 is more noticeable: $E_0/E_1 = 0.984$. The same value E_0/E_1 is accepted for the ratio γ'/γ in our formulas.

REFERENCES

1. Hass J, Varchon F, Milla'n-Otoya JE et al. Why Multilayer Graphene on 4H-SiC 000_1 Behaves Like a Single Sheet of Graphene. *Phys. Rev. Lett.*, 2008, 100:125504–10.
2. Hara H, Sano Y, Arima K, Kagi K, Murata J, Kubota A, Mimura H, Yamauchi K. Catalyst-referred etching of silicon. *Science and Technology of Advanced Materials*, 2007, 8:162–165.
3. Fujii M, Tanaka S. Ordering Distance of Surface Nanofacets on Vicinal 4H-SiC(0001). *Phys. Rev. Lett.*, 2007, 99:016102.
4. Davydov SY. On the charge transfer in the system of adsorbed molecules graphene monolayer–SiC-substrate. *Semiconductors,* 2011, 45(5):629-633 (in Russ.).
5. Davydov SY, Lebedev AA, Posrednik OV. *Vvedenie v fiziku nanosystem* [Introduction to physics of nanosystems]. S.-Petersburg, SPbGETU "LETI" Publ., 2009, 112 p.
6. Castro-Neto AH, Guinea F, Peres NM et al. The electronic properties of graphene. *Rev. Mod. Phys.*, 2009, 81:109. arXiv.org > cond-mat > arXiv:0709.1163.
7. Norimatsu W, Kusunoki M. Formation process of graphene on SiC(0001). *Physica E*, 2010, 42:691-694.
8. Alekseev NI, Luchinin VV, Charykov NA. Initial Stage of the Epitaxial Assembly of Graphene from Silicon Carbide and Its Simulation by Semiempirical Quantum Chemical Methods: Carbon Face. *Russ.Journ. of Phys. Chem. A*, 2013, 87(10):1709-1720 (in Russ.).
9. Alekseyev NI. *Modelirovanie protsessov formirovaniya uglerodnykh nanomaterialov. Grafen, nanotrubki, fullereny* [Simulation of processes of formation of carbon nanomaterials. Graphene, nanotubes, fullerenes]. S.-

Petersburg, SPbGETU "LETI" Publ., 2014, 292 p.
10. Hicks J, Shepperd K, Wang F, Conrad EH. The structure of graphene grown on the SiC (000—1) surface. *J.Phys.D. Applied Physics*, 2012, 45(15):154002.
11. Brenner DW. Empirical potential for Hydrocarbons for Use in Simulating the Chemical Vapor Deposition on Diamond Films. *Physical Review B,* 1990, 42:9458-9471.
12. Popov VV, Polischuk OV, Davoyan AR, Ryzhii V, Otsuji T, Shur MS. Plasmonic terahertz lasing in an array of Gr nanocavities. *Phys. Rev. B,* 2012, 86:195437.